Equilibrium Chemistry Calculations for Lean and Rich Hydrocarbon-Air Mixtures.

S. M. Aithal
Mathematics and Computer Science Division, Argonne National Laboratory,
9700 S. Cass Ave., Argonne, IL 60439, USA

Phone # 630-252-3164, e-mail: aithal@mcs.anl.gov

Abstract: Chemical equilibrium calculations provide useful estimates of combustion products in a wide range of reacting flow systems. Equilibrium computations are widely used in computing finite-rate NO emissions in internal combustion engines. Equilibrium chemistry computations can also provide useful information in comparing emissions of engines with different additives such as natural gas or methanol. This paper describes a fast, robust method to compute equilibrium concentrations of combustion products by using a set of twenty species relevant to a wide range of combustible fuel-additive-air mixtures, using the equilibrium constant method. The reaction set included species such as C, C_2H_2 and HCN believed to be responsible for soot formation in rich fuel-air mixtures. An adaptation of Newton-Raphson method was used for solving the highly nonlinear system of equations describing the formation of equilibrium products in reacting fuel-additive-air mixtures. The effect of temperature, pressure, and composition for various fuel-additive-air mixtures was studied. The modified Newton-Raphson scheme was found to be a robust and fast method for computing chemical equilibrium concentrations for a wide range of operating conditions such as temperature, pressure, and composition of fuel-additive-air mixtures. This general-purpose equilibrium solver was applied to study equilibrium compositions of rich and lean-mixtures fuel-additive air mixtures of interest to next generation automotive engines and combustors. The equilibrium solver was coupled to a quasi-dimensional engine code in order to predict concentrations of emissions such as NO, NO_2,

C_2H_2, CO and HCN. Temporal variation of the equilibrium combustion products in spark-ignited and diesel engines were obtained using this method. It was seen that the equilibrium NO mole fraction (expressed in PPM) a few-crank angle degrees after the end of combustion compared well with experimental data for both spark-ignited and diesel engines. It was also seen that the equilibrium CO mole fraction predicted experimental trends; however the quantitative values of engine-out CO was higher than the equilibrium value by about an order of magnitude.

Keywords: equilibrium, dual-fuel, NO, emissions, Newton-Raphson

Nomenclature

G	molar Gibbs free energy (J/mole)
k_p	equilibrium constant
P	pressure (N/m^2)
P_a	partial pressure
$P(\theta)$	cylinder pressure at crank angle θ (N/m^2)
R_g	gas constant (J/kg-K)
R_u	universal gas constant (J/K)
$T(\theta)$	average cylinder temperature at crank angle θ (K)
$V(\theta)$	cylinder volume at crank angle θ (m^3)
x_k	mole fraction of the k^{th} species

Greek Symbols

ϕ	equivalence ratio
θ	crank angle
υ	stoichiometric coefficient

Abbreviations

BDC	bottom dead center
CAD	crank angle degrees
EGR	exhaust gas recirculation
EOC	end of combustion
EVO	exit valve open
PPM	parts per million
TDC	top dead center

1 Introduction

Combustion of hydrocarbons in power-generating equipments, such as gas turbines or internal combustion engines in automobiles, is a major source of air pollution. The combustion products formed from burning fuel-air mixtures contain oxides of nitrogen (NO, NO_2, and N_2O) along with CO, CO_2, and other organic compounds that are unburned or partially burned hydrocarbons. The relative amounts of these pollutants, usually on the order of several hundred parts per million (PPM), depend on various factors including composition of the fuel-air mixture and the operating conditions. Optimizing performance (power and efficiency), while minimizing emissions such as NO_x and soot, leads to conflicting design constraints, hence accurate prediction of these emissions is an important consideration in the design of engines and combustors. Development of fast and robust tools for computing engine-out NO_x can aid the design/analyses/optimization of not only existing engines but also newer engine designs based on a variety of fuel-additive-air mixtures (also called flexible fuel engines) [1, 2]. In these flexible fuel engines, the main fuel can be gasoline or diesel, and the additives can be natural gas

(methane), hydrogen, acetylene, or alcohols (methanol or ethanol). A comparison of the emission characteristics of different fuel-additive combinations can help in the design and development of such flexible-fuel engines.

Concentrations of emissions such as NO_x, CO, soot, UHCs among others can be computed by using finite-rate chemistry. Finite-rate chemistry calculations require the use of an appropriate mechanism (set of elementary reactions and their associated reaction rate constants) to describe the soot/CO/NO_x formation process with reasonable accuracy. Careful attention must be paid to the size of the time-step and initial conditions to ensure the stability and accuracy of the time-marching process. These requirements greatly increase the computational complexity and time required for solution. In order to reduce the computational complexity of full finite-rate chemistry computations, several simplifying assumptions can be made to derive rate-controlled expressions for the formation of NO and CO [3, 4]. As described in Ref. [3], the rate-controlled expression for NO formation assumes equilibrium concentrations of O, O_2, OH, H and N_2 computed at the local pressure and temperature in the postflame gas. Similarly, Ref. [4] computes rate-controlled CO concentrations using equilibrium concentrations of species (CO, CO_2, O_2, H_2O, H_2, N_2) in the source terms. Simplified rate-controlled computations of NO as described in Ref. [3] are widely used in quasi-dimensional engine modeling codes and are also being used for other fuel-additive air mixtures (methane-hydrogen) as described in Ref. [4]. The source terms (RHS) for the rate-controlled equations for NO and CO require the equilibrium values of various combustion products. Since the engine temperature and pressure vary continuously throughout the engine cycle, temporal variation of NO (or CO) using the rate-controlled expressions require equilibrium computations to be done very often (usually every crank angle degree - CAD). Equilibrium computations performed using look-up tables can be

cumbersome and computationally expensive. Based on the above-mentioned considerations, a fast, robust tool for computing equilibrium concentrations of combustion products can greatly aid the design, development and analyses of new engine operating regimes, and engines fuelled by different fuel blends.

Chemical equilibrium of a closed reacting system at a given pressure and temperature can be computed by minimizing the Gibbs free energy of the system or by using the approach of equilibrium constants using a set of reactions [5]. While these two formulations are equivalent and reduce to the same number of iteration equations [5 and references therein], each approach has its advantages and disadvantages. Minimization of the Gibbs free energy involves treating each species independently and does not require a set of reactions to be prescribed a priori. The details of the problem formulation and implementation using this approach are explained in [5]. In addition to these two main techniques, the element potential method can also be used for equilibrium computations, especially for multi-phase systems. STANJAN is an interactive computer program for chemical equilibrium analyses of based on the element potential method [6]. For most combustion problems of interest to engineering applications, however, the equilibrium constant method is easier to formulate and implement. More important, the method can be easily coupled to computational fluid dynamics (CFD) and/or quasi-dimensional codes that compute temperature and pressure in combustors.

Computation of equilibrium composition of a large set of species is a daunting task. The coupled system of equations describing the formation of products is highly non-linear and hence very difficult to converge using traditional numerical schemes such as the Newton-Raphson method. Due to this reason, several authors have studied equilibrium chemistry calculations using a small set of species (typically 6–13) [7-11, and references therein]. Rashidi [7] studied a

system with 13 species. Sample results were presented for hydrocarbons with an H/C ratio of 2, for a set of prescribed temperature and pressure. The numerical approach involved separating the species into two groups: species with relatively large concentrations (CO_2, H_2O, CO, H_2, O_2, and N_2) and species with lower concentrations (OH, NO, O, H, N_2O, NO_2, and N). Concentrations of those species with high values were determined first, by using the Newton-Raphson method. Following this step, the remaining species were determined with the successive substitution method. The two methods were iterated alternatively until the change in values was small. Details of the initial conditions or the total computational time were not explicitly described. This method is likely to be unsuitable for computing the temporal variation of species concentrations in engines, however, since the initial charge consists of a fuel-air mixture with little or no CO_2, H_2O, and H_2 (unless exhaust gas recirculation (EGR) is used). Furthermore, for stoichiometric and rich mixtures, O_2 concentrations tend to zero at equilibrium and hence cannot be included in the list of species with large concentrations. While the methodology presented in [7] can be used for certain types of equilibrium computations, it might not be appropriate in studying temporal variation of equilibrium products during an actual engine cycle.

Rakopoulos et al. [8] used 11 species to describe the combustion products of diesel engines. The diesel fuel was modeled as n-dodecane. The 11x11 system of nonlinear equations was reduced to a 4x4 system by algebraic manipulation. The resulting 4x4 system was solved by using the Newton-Raphson method to obtain equilibrium concentration of the products. Results for a range of temperature, pressure, and equivalence ratios were presented for n-dodecane. The solution procedure of reducing the 11x11 system of equations to a 4x4 system of equations used in [8] can be cumbersome, especially if one is interested in studying a wide-variety of fuel-additive air mixtures, thus limiting its utility as a general-purpose design tool. References [7-8]

present sample results of the equilibrium products of hydrocarbon combustion, but neither of the works discuss the applicability of their techniques to general fuel-additive air mixtures or in interpreting actual engine data.

This work is primarily focused on developing a fast, robust, and general-purpose tool to compute the equilibrium products for a wide-range of fuel-additive-air mixtures of relevance to a range of engines and combustors. The numerical tool developed in this work can be used to compute the temporal variation of equilibrium products of an engine powered by traditional fuels such as gasoline and diesel or various fuel-additive mixtures. The tool can also be coupled to CFD codes to compute soot precursors in internal combustion (IC) engines [12] or equilibrium NO concentration in other combustors [13]. In order to accomplish these goals, a general set of 20 species relevant to a wide range of lean and rich combustion systems was used (see Table 1). Three species, namely C, HCN and C_2H_2, believed to be important in the process of soot formation [14] were also included so as to enable the study of fuel-rich mixtures. The numerical framework developed in this work allows the user to study equilibrium composition of any fuel-additive mixture, where the fuel is of the form C_xH_y and the additive is of the form $C_{x1}H_{y1}O_{z1}$ (or $C_{x1}H_{y1}$) without any code modification. A modified Newton-Raphson scheme was used to solve the entire 20x20 system of equations using 4 element conservation equations and 16 non-linear equations shown in Table 2. The methodology used in this work does not require the use of hybrid solution methods as in [7] or an ad-hoc reduction of the non-linear equations as in [8], thus enhancing its utility as a design tool. This work also examined the equilibrium mole fractions of NO and CO a few crank-angle degrees after end of combustion (EOC), when NO formation is believed to be frozen. By comparing engine-out NO and CO emission with equilibrium mole fractions of NO and CO a few CAD after EOC, it is possible to assess the

applicability of equilibrium computations for obtaining quick estimates of NO_x and CO/soot emissions in IC engines.

This paper is organized as follows. Section 2 discusses the set-up and solution methodology of the system of non-linear equations used in this work. Section 3 discusses verification and validation of the solver and details regarding the robustness and computational time. Section 3 also discusses the applications of the numerical tool developed in this work in studying equilibrium concentrations of various fuel-additive air mixtures and also in analyzing emissions data in spark-ignited and diesel engines. Section 4 presents important conclusions and observations about this work.

2 Method of solution:

The details of computing equilibrium compositions of ideal gas mixtures using the equilibrium constant method are explained in standard thermodynamic texts [15] and are briefly described below for the benefit of the reader.

Given a chemical reaction of the form

$$\upsilon_a A + \upsilon_b B \leftrightarrow \upsilon_c C + \upsilon_d D \tag{1}$$

the equilibrium constant k_p can be written as

$$k_p = \frac{(P_c)^{\upsilon_c}(P_d)^{\upsilon_d}}{(P_a)^{\upsilon_a}(P_b)^{\upsilon_b}} \tag{2}$$

Since the partial pressure of species A is related to the mole fraction (x_a) as

$$P_a = x_a P \tag{3}$$

one can write the constant as

$$k_p = \frac{(x_c)^{\upsilon_c}(x_d)^{\upsilon_d}}{(x_a)^{\upsilon_a}(x_b)^{\upsilon_b}} P^{\upsilon_c+\upsilon_d-\upsilon_a-\upsilon_d=} \tag{4}$$

Following the treatment in standard thermodynamic textbooks,

$$\ln k_p = \frac{-1}{R_u T}\sum_{1}^{s} \upsilon_i \left(\Delta G_f^{\circ}(T)\right)_i \tag{5}$$

where $\Delta G(T)_i$ was computed by using the procedure outline in [16].

As shown in Table 1, C_xH_y, represents the fuel (such as diesel, which is modeled as n-heptane), and $C_{x1}H_{y1}O_{z1}$ represents an additive (such as CH_4 or CH_3OH). The numerical framework used in this work was set up such that the user specifies the values of x, y, x_1, y_1, and z_1, so as to identify the fuel and additive. The temperature-dependent thermophysical quantities, namely, entropy and enthalpy of individual species were computed using CHEMKIN coefficients. For each reaction given in Table 2, the reaction rate was calculated at the prescribed temperature and pressure (P) as shown in Eq. (5). The set of 20 equations corresponding to the 20 species used in this work consist of 4 element balance (atom conservation) equations for C, H, O, and N and 16 non-linear equations describing the relationship between the mole-fractions of the various species and the equilibrium rate constants as described in Eq. (2) (see Table 2).

The element balance equations of C, H, O and N can be written as

$$N_c = xN_{fuel} + x_1N_{additive} + N_{CO2} + N_{CO} + xN_{CxHy-1} + N_{HCN} + N_C + 2N_{C2H2}$$

$$N_h = yN_{fuel} + y_1N_{additive} + 2N_{H2O} + N_{OH} + N_H + 2N_{H2} + N_{HO2} + (y-1)N_{CxHy-1} + N_{HCN} + 2N_{C2H2}$$

$$N_o = z_1N_{additive} + 2N_{O2} + 2N_{CO2} + N_{H2O} + N_O + N_{NO} + N_{OH} + N_{N2O} + N_{CO} + 2N_{NO2} + 2N_{HO2}$$

$$N_n = 2N_{N2} + N_N + N_{NO} + 2N_{N2O} + N_{CO} + N_{NO2} + N_{HCN}$$

where N_c, N_h, N_o and N_n are the total number or C, H, O and N atoms in the system under consideration. The 4 atom conservation equations shown above along with the 16 non-linear equations shown in Table 2, were used to obtain the concentration of each of the 20 species considered in this work. The system of 20x20 equations was solved using an adaptation of the Newton-Raphson method, which is described next.

The Newton-Raphson method is most commonly used to solve coupled non-linear equations. In its most common form a system of non-linear equations with N variables can be written as

$$\boldsymbol{F}(x_1, x_2, x_3, \ldots x_N) = 0 \tag{6}$$

The Taylor expansion of Eq. (6) can be written as

$$\boldsymbol{F}(\boldsymbol{x} + \delta\boldsymbol{x}) = \boldsymbol{F}(\boldsymbol{x}) + \boldsymbol{J}.\delta\boldsymbol{x} + O(\delta\boldsymbol{x}^2) \tag{7}$$

where

$$\boldsymbol{J}_{i,j} = \frac{\partial F_i}{\partial x_j}$$

Setting $\boldsymbol{F}(\boldsymbol{x}+\delta\boldsymbol{x}) = 0$, in Eq. (7) leads to

$$\boldsymbol{F}(\boldsymbol{x}) = -\boldsymbol{J}.\delta\boldsymbol{x} \tag{8}$$

Solution of the Eq. (8) yields the solution vector, $\boldsymbol{x}$. However, for large system of highly non-linear equations the textbook version of Newton-Raphson methods can have many convergence issues. This is especially true for combustion systems where the Jacobian can become ill-condition. This is largely on account of the fact that elements of the Jacobian matrix are products of reaction rate constants and partial pressures of various species. The initial mixture composition consists entirely of the fuel-additive air mixture with other species being zero, while the equilibrium system consists of non-zero values of all species considered in the system. The species concentrations in the equilibrium mixture span 8 to 10 orders of magnitude (see Tables 3-5). Hence the condition number of the matrix changes drastically during the course of the solution process. Furthermore, each element of the solution vector $\boldsymbol{x}$ should be greater than zero (since mole fraction of any species cannot be negative), which makes convergence of such systems extremely difficult. This fact can be illustrated by studying the numerical values of the reaction rate constants of typical combustion reactions.

Figure 1 shows the variation of the reaction rate constants of reactions 1, 11, 12 and 16 shown in Table 2. It is seen that the reaction rate constants can differ by over 100 orders of magnitude, thus making the Jacobian matrix extremely ill-conditioned. In order to develop a fast, robust

solver for a generalized fuel-additive air mixture an adaptation of the textbook version of the Newton-Raphson method was developed and tested.

For this work, the species composition vector (or solution vector comprising of species equilibrium composition) $\boldsymbol{x}$ consists of 20 elements corresponding to the 20 species, while the Jacobian is a 20x20 matrix. Eq. (8) was solved using the LU decomposition method using LAPACK routines to obtain $\delta\boldsymbol{x}$ where $\delta\boldsymbol{x}$ is the "correction" used to obtain the set of values for the next iteration. The subsequent iteration (iteration *n+1*) used updated values for the solution vector $\boldsymbol{x}$ as shown below

$$\boldsymbol{x_{n+1}} = \boldsymbol{x_n} + \alpha_n \delta \boldsymbol{x} \tag{9}$$

to solve Eq. (8). Computing an approximate Jacobian based on numerical finite differences can greatly slow down the computations, hence analytical expressions for each of the elements of the Jacobian and $\boldsymbol{F(x)}$ were used. Since the set of reactions shown in Table 2 are written in a generalized form using x, y, x_1, y_1, and z_1 to identify the fuel and additive, the analytical forms of the Jacobian and source terms are valid for all user-defined values of x, y, x_1, y_1, and z_1, thus making it a general-purpose design tool. An under-relaxation factor α was used in order to ensure that each element of the solution vector was non-negative during the course of the iteration procedure. The L^2 norm was computed for each iteration. If during a particular iteration, *n*, the L^2 norm was higher than the L^2 norm of the previous iteration, the under-relation factor was reduced by 10^{-3} or ($\alpha_{n+1}=\alpha_n - 10^{-3}$). The iteration procedure was terminated when the L^2 norm was below a prescribed convergence criterion. All simulations were started by setting $\alpha = 1$. Iterations for the Newton-Raphson scheme were terminated when the L^2 norm was below 10^{-25}. The use of analytical forms of the Jacobian matrix, optimized LAPACK routines for the solution of Eq. (8) makes the solution of the system of equation extremely fast. The use of an

under-relaxation factor based on the L^2 norm made the system robust (ensured convergence) for all cases presented in this work.

The methodology described above allows the user to test various fuel-additive combinations without any code modifications, thus making it a valuable design tool for analyzing rich and lean fuel-additive-air mixtures.

3 Results and Discussion

This section focuses on three aspects: verification of the Newton-Raphson solver, the computational time and robustness of the solver and various applications of the numerical tool. The primary application of this numerical tool is in understanding the impact of temperature, pressure and equivalence ratio on the formation of equilibrium products of combusting mixtures. Since the equilibrium composition of the combustion products includes species such as NO, CO, C_2H_2 and HCN, this numerical tool can also be used to compare emissive products from the combustion of various fuel-additive-air mixtures. Applicability of the use of equilibrium assumptions in estimating emissions (NO and CO/soot) in spark-ignited natural gas engines and dual-fuel diesel engines, is also discussed in this section.

3.1 Verification of the Newton-Raphson solver

A variety of fuel-additive air mixtures at various temperatures and pressures were used to rigorously test the solver. Results for pentane-methanol-air, pentane-methane-air and rich pentane-air mixtures at a range of temperatures (2200 K – 3200 K) and pressures (35 – 80 atm) are presented in Tables 3 to 5. These results demonstrate the ability of the Newton-Raphson solver to compute equilibrium concentrations of complex hydrocarbon mixtures over a range of

temperatures and pressures relevant to engine operating conditions. All computations were conducted by using the constant pressure, constant temperature constraint. As seen in Tables 3 to 5, the results computed by using the Newton-Raphson solver in this work are in excellent agreement with those computed by using STANJAN [17], thus verifying the accuracy of the Newton-Raphson solver.

3.2 Computation time required for the simulation

Robustness, computational time and wide-range of applicability are important considerations for design and analysis tools. These details for the present work are discussed next.

For lean fuel-additive-air mixtures, obtaining equilibrium concentrations at a prescribed temperature and pressure typically took about 10–20 iterations, requiring a total time of less than 1 millisecond on single-CPU 3 GHz machine. An entire sequence of 360 equilibrium calculations (conducted every CAD) for the compression/expansion stroke of a typical engine cycle took about 100 milliseconds. These computations were thus about 3 orders of magnitude faster than computations conducted with STANJAN/CHEMKIN, which take on the order of 3–15 seconds for a single equilibrium calculation at a given temperature, pressure and mixture composition.

Equilibrium calculations of rich mixtures took about 50–250 iterations, depending on temperature, pressure and operating conditions. The time required for computing the equilibrium concentration of a rich fuel-air mixture for a single prescribed value of temperature and pressure was on the order of 5–20 milliseconds. The Newton-Raphson solver used in this work was extremely robust.

Figure 2 shows the drop in residuals with iterations for a stoichiometric pentane-air mixture (ϕ=1) and a rich pentane-air mixture (ϕ=5) starting from an initial mixture consisting only of pentane and air (oxygen and nitrogen). It is seen that the residuals drop by about 150 orders of magnitude in about 50 iterations for the stoichiometric case, whereas it takes about 250 iterations for the fuel-rich case. No numerical instability or divergence was observed for a wide range of temperatures, pressure and mixture compositions studied in this work.

From the above discussion, it is seen that the Newton-Raphson method is robust and computationally fast for the system of 20x20 coupled equations considered in this work. Since the methodology allows the user to define the fuel and additive as inputs, the same solver can be used to study a range of fuel-additive-air mixtures and hence can be used as a reliable design tool. This work demonstrated that the Newton-Raphson method can be used to achieve good numerical stability/robustness and short computational times (on the order of milliseconds) without resorting to ad-hoc reduction of the system of non-linear equations as in [8] or using a hybrid method as in [7] for a range of fuel-additive-air mixtures, thus demonstrating the wide-range applicability of this work.

3.3 Applications:

The numerical tool developed in this work was used to compute equilibrium products for a wide variety of hydrocarbon-air mixtures at different temperatures and pressures. The chosen hydrocarbon-air mixtures, temperatures and pressure were representative of different fuel-additive air mixtures used as engine fuels at different engine operating conditions. Three applications are described next.

3.3.1 Equilibrium concentration of fuel-rich hydrocarbon mixtures:

Modern diesel engines use exhaust-gas recirculation (EGR) for NO_x control. Introduction of EGR leads to reduced flame temperature and hence a reduction of NO_x. However, the combined effect of reducing charge-gas oxygen and temperatures due to EGR leads to incomplete combustion and increased particulate matter emissions. The numerical tool developed in this work was used to study important combustion products in fuel-rich (equivalence ratio > 1) n-heptane-air and pentane-air mixtures. These mixtures were chosen because most theoretical computations use n-heptane as a diesel fuel surrogate [12]. Incomplete combustion of n-heptane can lead to the formation of lower hydrocarbons such as pentane (amongst other hydrocarbons). Unburned fuel (n-heptane) and partially burned fuel such as pentane lead to the formation of particulate matter in fuel-rich pockets in the combustion chamber. Figure 3 shows important species concentrations in fuel-rich pentane and n-heptane mixtures at T = 2200 K and P = 80 atm. This particular temperature and pressure is representative of conditions in a diesel engine operating near full-load close to top dead center (TDC) and hence chosen for investigation. The equilibrium composition of combustion products for both pentane and n-heptane exhibit similar characteristics. As expected, there is a marked increase in CO and H_2 (almost 2 orders of magnitude) as the equivalence ratio φ increases above 2, with a corresponding drop in CO_2 and H_2O. It is also seen that there is a marked increase in the concentration of HCN and C_2H_2 beyond an equivalence ratio of 3. C_2H_2 is believed to be a precursor in soot formation and hence its concentration is important in understanding the effect of equivalence ratio on soot formation. Figure 4 shows the effect of temperature and pressure on the formation of C_2H_2 and HCN in fuel-rich n-heptane air mixtures under 2 different operating conditions, namely, T = 1500 K, P = 35 atm and T = 2200 K, P = 80 atm. The engine temperature and pressure are close to 1500 K

and 35 atm after the beginning of the fuel injection (SOI) in a typical diesel engine, whereas T = 2200 K, P = 80 atm corresponds to conditions near TDC toward the end of the fuel injection process. During the initial phase of droplet break-up and fuel combustion, the equivalence ratio in certain regions of the chamber is believed to be between 2 and 5 and hence chosen for this study. At equivalence ratios below $\phi = 3$, formation of HCN and C_2H_2 is negligible. However, the concentration of these species increases dramatically beyond $\phi = 3$. As expected, at lower temperatures and pressures, the equilibrium concentration of C_2H_2 is higher, but it drops as the temperature and pressure increase during the compression stroke. At higher temperatures and pressures, the concentration of HCN increases as compared to its value at a lower temperature. These equilibrium computations qualitatively capture the trends reported in literature on the effect of EGR on soot formation and hence can aid in evaluating trade-offs in NO_x and soot formation.

3.3.2 Effect of additives on equilibrium NO formation in dual-fuel engines:

Dual-fuel engines run on a variety fuel-additive air mixtures. Dual-fuel diesel engines run using CH_4 and also other gaseous fuels such as C_2H_2, H_2, and CH_3OH. Experimental studies of such engines have been reported by various groups [19-21]. These dual-fuel engines have many advantages. For instance, dual-fuel diesel engines using natural gas operate on both natural gas and diesel fuel simultaneously. The majority of the fuel burned is natural gas, whereas diesel fuel is used as a pilot to ignite the mixture. This strategy allows retention of the diesel compression ratio and the associated higher efficiency while burning cheap and clean natural gas. Dual-fuel engines can run on either liquid natural gas or compressed natural gas. Both fuels have relatively high octane numbers, which lead to performance improvements. Furthermore, engines running

natural gas with diesel typically have 20% to 30% less CO_2 emissions. Dual-fuel engines can also be operated in the straight diesel mode, if need be, which greatly enhances its utility as a flexible fuel engine. Given these desirable features of dual-fuel engines, their design and optimization would benefit greatly if designers could evaluate the relative effects of the fuel-type, engine load, and speed on emissions. For instance, Lakshmanan and Nagarajan [20] report a 24% increase in NO emissions with a C_2H_2/diesel operation, while Papagiannakis et al. [19] report a reduction in NO with a CH_4/diesel operation. By studying the effect of temperature on the diesel-additive combination, some estimates of the impact of fuel-additive ratio on NO emissions can be obtained.

Figure 5 shows the effect of temperature on the equilibrium NO for various combinations of n-heptane and natural gas (CH_4). The number of moles of n-heptane and CH_4 was varied so as to maintain a constant value of enthalpy corresponding to a case of neat stoichiometric diesel operation (1 mole of n-heptane, 0 moles of CH_4). It is seen that a stoichometric n-heptane/CH_4 mixture with 0.1 moles of n-heptane and 1.457 moles of CH_4 has about a 5% lower NO concentration at conditions close to TDC (2000–2200 K) as compared to the case with neat diesel. As expected, an intermediate case with 0.5 moles of n-heptane and 0.78 moles of CH_4 results in less reduction of NO concentration.

3.3.3 Comparison of equilibrium NO and CO concentrations with engine data

This section discusses two case-studies which compare the temporal variation of equilibrium NO and CO mole-fractions with corresponding engine-out values in automotive engines. The two cases considered were large-bore stationary natural gas engines and dual-fuel diesel engines. The finite-rate computations of NO and CO described in Ref. [3-4], assume the C-H-O system to

be in equilibrium [22]. The temporal variation of NO is obtained by a solution of an ordinary differential equation (ODE) describing the time-rate-of-change of NO. There are several simplifying assumptions used to derive the finite-rate equation for NO formation and Ref. [3] points out that the NO formation rate could increase or decrease. The authors in Ref. [22] point out that the good agreement between model predictions and engine-out NO reported in [3] is fortuitous. Given these considerations, it is instructive to compare the equilibrium composition of NO (and CO) at temperature and pressure conditions a few crank angle degrees after EOC with engine-out NO and CO data. Such a comparison would enable one to assess the accuracy of using equilibrium assumptions at temperature and pressure conditions a few crank angle degrees after EOC (where NO formation is believed to be frozen), for estimating engine-out NO and CO values under actual engine operating conditions.

3.3.3.1 Full-cycle NO and CO calculations in natural gas engines:

Stationary large-bore engines fueled by natural gas are used in applications such as power generation and gas transmission. Since such engines are used for long durations, optimizing their performance and emissions is essential. NO and CO emissions from such engines can be analyzed by using the strategy outlined below and can be useful in assessing various NO abatement strategies. Knowing the temporal variation of pressure (from engine data), engine geometry, and flow rates of the fuel and air, one can compute the temporal variation of average temperature in the engine cylinder. The average cylinder temperature at a given crank angle θ is given by $T(\theta) = \frac{P(\theta)V(\theta)}{mR_g(\theta)}$, where $R_g(\theta)$ is the gas constant and m is the total mass of the working fluid (unburned fuel, air, and combustion products) at a given crank angle. Knowing

the composition of the fuel-air mixture at the start of the compression stroke, along with the temporal variation of pressure and temperature, one can obtain the equilibrium composition of the combustion products at each crank angle. The species concentration at each crank angle serves as the initial concentration for the calculation of equilibrium products at the pressure and temperature at the next crank angle. Figure 6 (a) shows experimental pressure profiles for the 0% nitrogen enriched air (NEA) spark-ignition case discussed in [18] for two equivalence ratios, $\phi = 1.0$ and $\phi = 0.65$. Figure 6 (b) shows the temporal variation of average cylinder temperature calculated by using the procedure discussed above. As explained above, the average cylinder temperature is proportional both to the cylinder pressure and mass of the working fluid. The case with $\phi = 0.65$ has a higher air mass and hence a lower overall average temperature than that of the $\phi = 1.0$ case, despite the higher cylinder pressure shown in Figure 6 (a). Methane (CH_4) was used to represent natural gas in the equilibrium chemistry computations. As seen in Figure 6 (c) the equilibrium NO production follows the temperature variation, with NO values for the $\phi = 1$ case being higher than the $\phi = 0.65$ case. As the temperature and pressure of the working fluid decrease during the expansion stroke, the NO concentration drops sharply. The high pressure and temperature near TDC allow the reaction kinetics to reach near equilibrium concentrations. The NO composition is believed to freeze a few crank-angle degrees after combustion is complete (typically around 35°–50° ATDC). For lean mixtures, the combustion duration is longer than that for near-stoichiometric mixtures. The NO concentration shown in (c) around 35° ATDC is about 3000 PPM for $\phi = 1$ and about 2000 PPM for $\phi = 0.65$ at 50° ATDC. These values match closely with the engine-out NO reported in [18]. Figure 6 (d) shows the temporal variation of CO throughout the engine cycle for several values of equivalence ratios. At the end of combustion ($\theta > 35$ ATDC), there is a steep drop in the CO concentration as the equivalence

ratio changes from stoichiometric to fuel-lean (ϕ = 0.9), followed by a less pronounced drop in CO concentration for smaller values of the equivalence ratio ϕ. These characteristics do not agree well with the engine-out CO measurements reported in [18]. Experimental data in [18] shows that the overall drop in engine-out CO from φ = 1 to ϕ = 0.65 is about an order of magnitude, whereas equilibrium computations show a much larger drop in CO at any given crank angle, as shown in Figure 6 (d). For instance, at a crank angle of 40°, the concentration of CO is about 6000 PPM for ϕ = 1, whereas it is about 20 PPM at ϕ = 0.65. This observation suggests that CO formation and depletion is strongly dependent on chemical kinetics and hence cannot be well predicted by equilibrium assumptions. Equilibrium concentrations of C, C_2H_2, CH_3, and HCN were also negligible (< 1.0E-5 PPM) for temperatures and pressures typical of near-TDC conditions (T = 2500 K and P = 50 atm) and also at conditions typical of exhaust valve open (EVO) conditions (T = 1000K and P = 5 atm). These observations suggest that equilibrium assumptions may be unsuitable for predicting engine-out concentrations of CO, soot, and soot-forming precursors (C, C_2H_2, CH_3) in lean mixtures.

3.3.3.2 Full-cycle NO and CO calculations in dual-fuel diesel engines:

The equilibrium chemistry solver can also be used to analyze and estimate NO emissions for actual engine operating conditions in dual-fuel diesel engines. Sample calculations were conducted to assess NO concentrations predicted by equilibrium computations with experimental data reported in [19]. Using the geometrical details of the single-cylinder, naturally aspirated engine, the initial cylinder composition was computed at bottom dead center (BDC) for various values of diesel fuel supplementary ratio (x) and total relative air-fuel ratio (λ) as defined in [19]. Figure 7 shows a comparison of NO concentration predicted by the equilibrium solver with

experimental data reported in [19] corresponding to an engine speed of 1500 RPM, for three loads (BMEP). Since details about the temporal variation of pressure are not described in [19], equilibrium computations were conducted at a pressure of 20 atm. It was verified that the NO concentrations were a weak function of pressure at a given temperature (about 1.5% difference over a pressure difference of 10 atm). At each value of x and λ (corresponding to a given load), equilibrium computations were performed for a range of temperatures from 1000 K to 2000 K. It was seen that the NO concentrations at temperatures of 1250 K, 1350 K, and 1450 K for engine loads (BMEP) of 1.2, 2.4, and 3.7 bar, respectively, matched values reported in [19]. These temperature values are representative of average gas temperature in the diesel engine a few crank-angle degrees after fuel combustion is complete. At higher engine loads, the exhaust temperature is higher as reported in [19]. Hence the value of temperature corresponding to which equilibrium NO matches experimental data also increases.

Figure 8 shows CO concentration over a range of temperatures for three values of load and mixture composition (x and λ). The CO concentration predicted using equilibrium assumptions is less than 1 g/kWh even for temperatures as high as 2000 K, whereas the CO concentrations reported in [19] lie between 1 and 100 g/kWh. This result is consistent with the earlier observation that equilibrium assumptions are not suitable for CO concentrations, especially for fuel-lean conditions. Concentrations of C, C_2H_2, HCH, and C_7H_{15} were also negligible (similar to equilibrium compositions noted with the natural gas engine computations).

4 Conclusions

Chemical equilibrium calculations were conducted with a set of species relevant to a wide-range of combustible fuel-additive-air mixtures using the equilibrium constant method. The Newton-

Raphson method was found to be a fast and robust technique for solving the system of nonlinear equations describing the formation of equilibrium products in combusting mixtures. Equilibrium chemistry computations yielded results that agree well with NO_x formation trends observed in diesel and SI engines. It was also seen that equilibrium computations for CO did not match well with experimental data. Similarly, equilibrium concentrations of species believed to be precursors in soot formation such as C, C_2H_2, and HCN were found to be negligible in both the cases studied in this work. These observations suggest that equilibrium computations have the potential to provide good estimates of engine-out NO_x in a wide variety of engines and to assist in the evaluation of various NO_x abatement strategies. The results of this work also suggest that prediction of CO and soot in fuel-lean conditions might require more detailed finite-rate chemical kinetic computations.

Acknowledgments: The submitted manuscript has been created by UChicago Argonne, LLC, Operator of Argonne National Laboratory ("Argonne"). Argonne, a U.S. Department of Energy Office of Science laboratory, is operated under Contract No. DE-AC02-06CH11357.

References

1. Wallner, T., Miers, S. A., McConnell, S., "A comparison of ethanol and butanol as oxygenates using a direct-injection, spark-ignition engine," J. Eng. Gas Turbines Power 131(3) (2009).
2. Wallner, T., Frazee, R., "Study of regulated and non-regulated emissions from combustion of gasoline, alcohol fuels and their blends in a DI-SI engine," SAE paper 2010-01-1571, 2010.
3. Heywood, J. B., *Internal Combustion Engine Fundamentals,* McGraw-Hill, New York, 1988.

4. F. Perini, F. Paltrinieri, E. Mattarelli, "A quasi-dimensional combustion model for performance and emissions of SI engines running on hydrogen–methane blends", Int. J. of Hydrogen Energy, Vol. 35 (10), 2010, pp 4687-4701.
5. Gordon, S. and McBride, B. I., "Computer program for calculation of complex chemical equilibrium compositions and applications," NASA Reference Publication 1311, Oct. 1994.
6. W. C. Reynolds, "STANJAN: interactive computer programs for chemical equilibrium analysis", Stanford University. Dept. of Mechanical Engineering. Thermosciences Division, 1981.
7. Rashidi, M, "Calculation of equilibrium composition in combustion products," Chem. Eng. Technol. 20 (1997) 571–575.
8. Rakopoulos, C. D., Hountalas, D. T., Tzanos E. I., G. N. Taklis, "A fast algorithm for calculating the composition of diesel combustion products using 11 species chemical equilibrium scheme," Advances in Engineering Software 19 (1994) 109-119.
9. Vickland, C. W., Strange, F. M., Bell, R. A., Starkman, E. S., "A consideration of the high temperature thermodynamics of internal combustion engines," Trans. SAE 70 (1962) 785 – 793.
10. Way, R. J. B., "Methods for determination of composition and thermodynamic properties of combustion products for internal combustion engines calculations," Inst. Mech. Engrs. 190 (1977) 687–697.
11. Olikara, C., Bofman, G. L., "A computer program for calculating properties of equilibrium combustion products with some applications to I.C. engines," SAE Paper 750468, 1975.
12. Som, S., "Development and validation of spray models for investigating diesel engine combustion and emissions", Ph.D. dissertation, University of Illinois at Chicago, 2009.

13. K. Khanafer, S.M. Aithal, Fluid-dynamic and NOx computation in swirl burners, Int. J. Heat Mass Transfer (2011),doi:10.1016/j.ijheatmasstransfer.2011.07.017
14. Tao, F. Srinivas, S., Reitz, R. D., Foster, D. E., "Comparison of three soot models applied to multi-dimensional diesel combustion simulations," JSME International Journal Series B 48(4) (2005) 671–678.
15. Van Wylen, G. J., Sonntag, R. E., "Fundamentals of classical thermodynamics", 2nd ed. John Wiley.
16. Kee, R. J., Rupley, F. M, Meeks E, Miller, J. A., "CHEMKIN-III: A FORTRAN chemical kinetics package for the analysis of gas-phase chemical and plasma kinetics," Sandia technical report SAND96-8216, 1996.
17. http://navier.engr.colostate.edu/tools/equil.html
18. Biruduganti, M., Gupta, S., Bihari, B., McConnell, S., Sekar, R., "Air separation membranes – an alternative to EGR in large bore natural gas engines," ASME Internal Combustion Engine 2009 spring technical conference paper ICES2009-76054, 2009.
19. Papagiannakis, R. G., Rakopoulos, C. D., Hountalas, D. T., Rakapoulos, D. C., "Emission characteristics of high speed, dual fuel, compression ignition engine operating in a wide range of natural gas/diesel fuel proportions," Fuel 89(7) (2010) 1397–1406.
20. Lakshmanan, T., Nagarajan, G., "Experimental investigation on dual fuel operation of acetylene in a DI diesel engine," Fuel Processing Technology 91(5) (2010) 496–503.
21. Lata, D. B., Misra, A., "Theoretical and experimental investigations on the performance of dual fuel diesel engine with hydrogen and LPG as secondary fuels," Int. J. Hydrogen Energy 35(21) (2010) 11918 –11931.

22. Ferguson, C. R, Kirkpatrick, A. T. “Internal Combustion Engines: Applied Thermosciences” 2nd Ed, John Wiley and Sons, NY, 2001.

Table 1: List of species

	Species*
1	C_xH_y (fuel)
2	$C_{x1}H_{y1}O_{z1}$ (additive)
3	O_2
4	CO_2
5	H_2O
6	N_2
7	N
8	O
9	NO
10	OH
11	H
12	N_2O
13	CO
14	H_2
15	NO_2
16	HO_2
17	C
18	HCN
19	C2H2
20	C_xH_{y-1}

*x and y are the number of carbon and hydrogen atoms in the hydrocarbon; x_1 and y_1, are the carbon and hydrogen atoms in the additive, while z_1 are the oxygen atoms in the additive.

Table 2: Elementary processes considered in this model

1	$\frac{1}{2}H_2 = H$	$k_1 = \frac{[H]}{[H_2]^{0.5}}\sqrt{P}$
2	$\frac{1}{2}O_2 = O$	$k_2 = \frac{[O]}{[O_2]^{0.5}}\sqrt{P}$
3	$\frac{1}{2}N_2 = N$	$k_3 = \frac{[N]}{[N_2]^{0.5}}\sqrt{P}$
4	$\frac{1}{2}H_2 + \frac{1}{2}O_2 = OH$	$k_4 = \frac{[OH]}{[H_2]^{0.5}[O]^{0.5}}$
5	$\frac{1}{2}N_2 + \frac{1}{2}O_2 = NO$	$k_5 = \frac{[NO]}{[N_2]^{0.5}[O]^{0.5}}$
6	$H_2 + \frac{1}{2}O_2 = H_2O$	$k_6 = \frac{[H_2O]}{[H_2][O_2]^{0.5}}(P)^{-0..5}$
7	$CO + \frac{1}{2}O_2 = CO_2$	$k_7 = \frac{[CO_2]}{[CO][O_2]^{0.5}}(P)^{-0.5}$
8	$NO + \frac{1}{2}O_2 = NO_2$	$k_8 = \frac{[NO_2]}{[NO][O_2]^{0.5}}(P)^{-0.5}$
9	$O_2 + \frac{1}{2}H_2 = HO_2$	$k_9 = \frac{[HO_2]}{[O_2][H_2]^{0.5}}(P)^{-0.5}$
10	$N_2 + \frac{1}{2}O_2 = N_2O$	$k_{10} = \frac{[N_2O]}{[N_2][O_2]^{0.5}}(P)^{-0.5}$
11	$C_xH_y + \left(x + \frac{y}{4}\right)O_2 = xCO_2 + \frac{y}{2}H_2O$	$k_{11} = \frac{[CO_2]^x[H_2O]^{0.5y}}{[C_xH_y][O_2]^{x+0.25y}}(P)^{(0.25y-1)}$
12	$C_{x1}H_{y1}O_{z1} + \left(x1 + \frac{y1}{4} - \frac{z1}{2}\right)O_2 = x1CO_2 + \frac{y1}{2}H_2O$	$k_{12} = \frac{[CO_2]^{x1}[H_2O]^{0.5y1}}{[C_{x1}H_{y1}O_{z1}][O_2]^{x1+0.25y1-0.5z1}}(P)^{(0.25y1-1+0.5z1)}$

13	$C_x H_y = C_x H_{y-1} + H$	$k_{13} = \frac{[C_x H_{y-1}][H]}{[C_x H_y]} P$
14	$2C_x H_{y-1} = xC_2 H_2 + (y - x - 1)H_2$	$k_{14} = \frac{[C_2 H_2]^x [H_2]^{(y-x-1)}}{[C_x H_{y-1}]^2} (P)^{(y-3)}$
15	$C_2 H_2 = 2C + H_2$	$k_{15} = \frac{[C]^2 [H_2]}{[C_2 H_2]} P^2$
16	$C_2 H_2 + N_2 = 2HCN$	$k_{16} = \frac{[HCN]^2}{[C_2 H_2][N_2]}$

Table 3: Verification of equilibrium composition of pentane-methanol mixture

Temperature (K)	3200
Pressure (atm)	35
C_5H_{12} (moles)	1
CH_3OH (moles)	0.1
O_2 (moles)	8.15
N_2 (moles)	30.644
All other species	1.0E-30

	Species	Equilibrium Mole Fraction (Current study)	STANJAN (Mole Fraction) [17]
1	C_5H_{12}	1.186889E-58	0.0000E+00
2	CH_3OH	3.108337E-12	6.4634E-14
3	O_2	1.790785E-02	1.7911E-02
4	CO_2	6.401841E-02	6.4002E-02
5	H_2O	1.165357E-01	1.1653E-01
6	N_2	6.902252E-01	6.9022E-01
7	N	6.506663E-06	6.5026E-06
8	O	4.830986E-03	4.8321E-03
9	NO	1.701193E-02	1.7019E-02
10	OH	1.936549E-02	1.9366E-02
11	H	5.280299E-03	5.2794E-03
12	N_2O	4.841432E-06	4.8389E-06
13	CO	5.227207E-02	5.2288E-02
14	H_2	1.250074E-02	1.2501E-02
15	NO_2	1.308406E-05	1.3075E-05
16	HO_2	2.694174E-05	2.6933E-05

Table 4: Verification of equilibrium composition of pentane-methane-air mixture

Temperature (K)	2500
Pressure (atm)	35
C_5H_{12} (moles)	1
CH_4 (moles)	1
O_2 (moles)	10
N_2 (moles)	37.6
All other species	1.0E-30

	Species	Equilibrium Mole Fraction (Current study)	STANJAN (Mole Fraction)
1	C_5H_{12}	4.725217E-67	0.0
2	CH_4	3.531725E-15	3.5264E-15
3	O_2	3.992629E-03	3.9936E-03
4	CO_2	1.052205E-01	1.0522E-01
5	H_2O	1.500578E-01	1.5006E-01
6	N_2	7.218287E-01	7.2183E-01
7	N	4.168169E-08	4.1642E-08
8	O	1.533250E-04	1.5334E-04
9	NO	3.184135E-03	3.1852E-03
10	OH	2.748469E-03	2.7484E-03
11	H	2.063659E-04	2.0628E-04
12	N_2O	9.032364E-07	9.0274E-07
13	CO	1.021927E-02	1.0223E-02
14	H_2	2.383271E-03	2.3828E-03
15	NO_2	2.105280E-06	2.1039E-06
16	HO_2	2.439475E-06	2.4386E-06

Table 5: Verification of equilibrium composition of rich pentane-air mixture ($\phi = 5$)

Temperature (K)	2200
Pressure (atm)	80
C_5H_{12} (moles)	5
CH_4 (moles)	0
O_2 (moles)	8
N_2 (moles)	30.08
All other species	1.0E-30

	Species	Equilibrium Mole Fraction (Current study)	STANJAN (Mole Fraction)
1	C_5H_{12}	4.725217E-67	0.0
2	CH_4	3.531725E-15	3.5264E-15
3	O_2	3.992629E-03	3.9936E-03
4	CO_2	1.052205E-01	1.0522E-01
5	H_2O	1.500578E-01	1.5006E-01
6	N_2	7.218287E-01	7.2183E-01
7	N	4.168169E-08	4.1642E-08
8	O	1.533250E-04	1.5334E-04
9	NO	3.184135E-03	3.1852E-03
10	OH	2.748469E-03	2.7484E-03
11	H	2.063659E-04	2.0628E-04
12	N_2O	9.032364E-07	9.0274E-07
13	CO	1.021927E-02	1.0223E-02
14	H_2	2.383271E-03	2.3828E-03
15	NO_2	2.105280E-06	2.1039E-06
16	HO_2	2.439475E-06	2.4386E-06

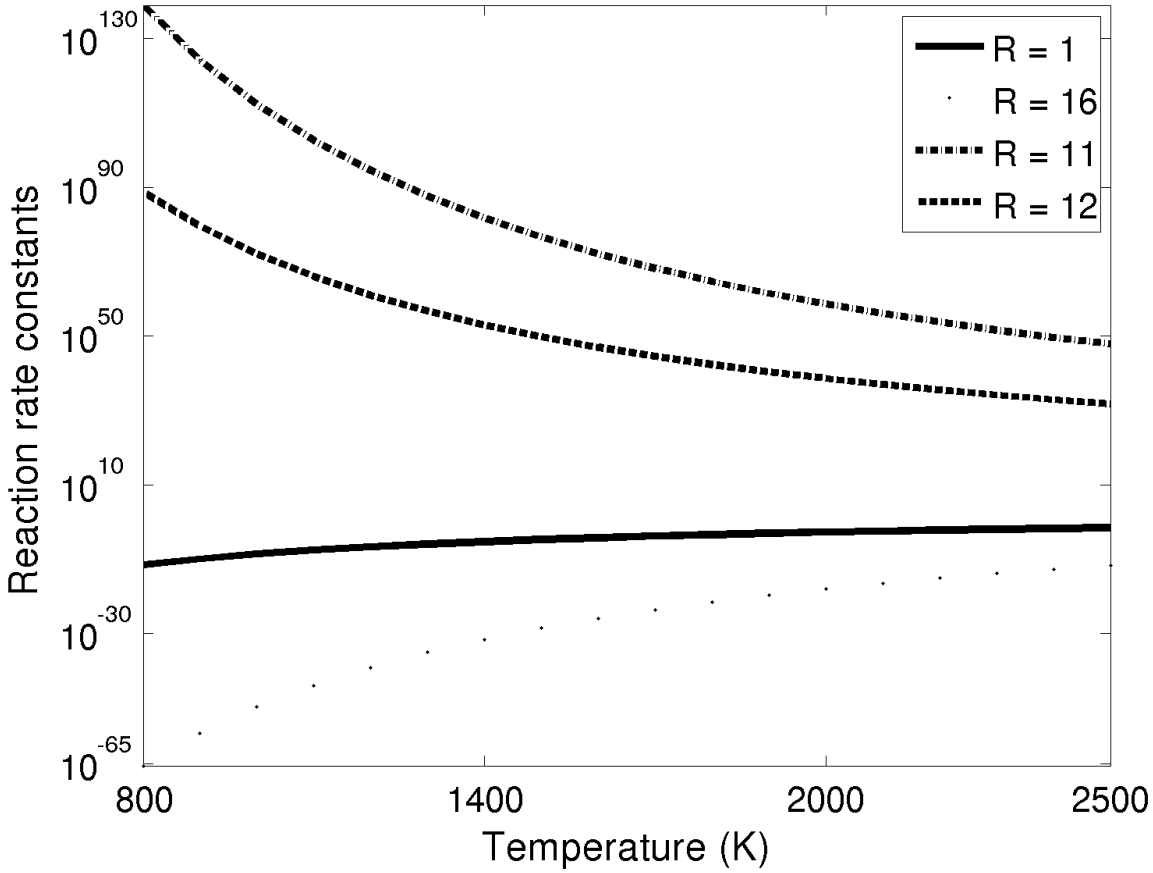

Figure 1: Variation of reaction rate constants with temperature.

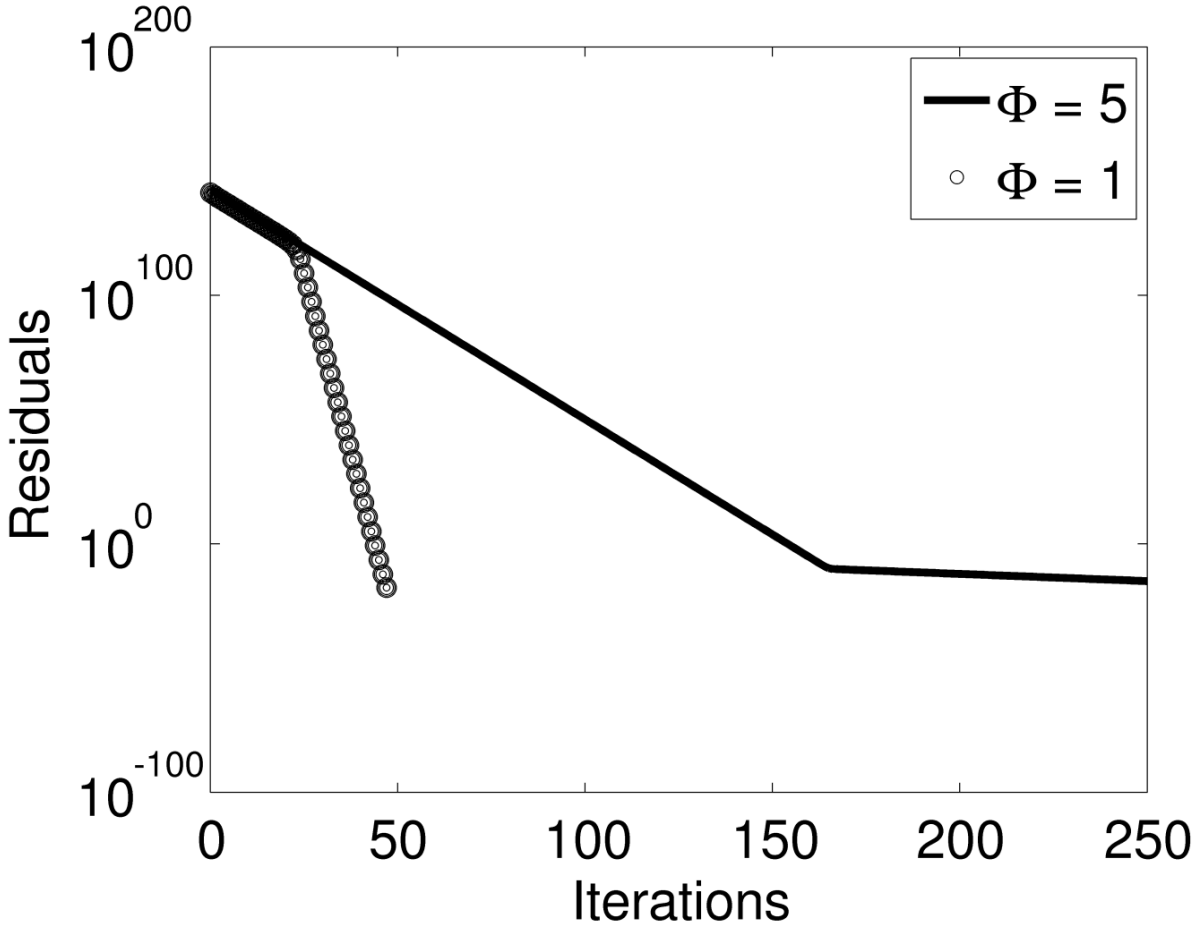

Figure 2: Variation of residuals with iterations for pentane-air mixtures.

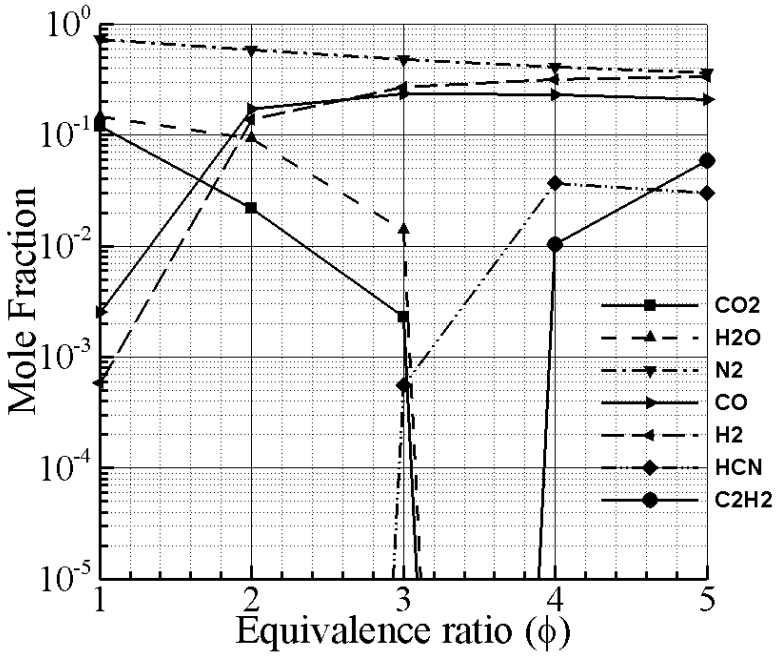

(a)

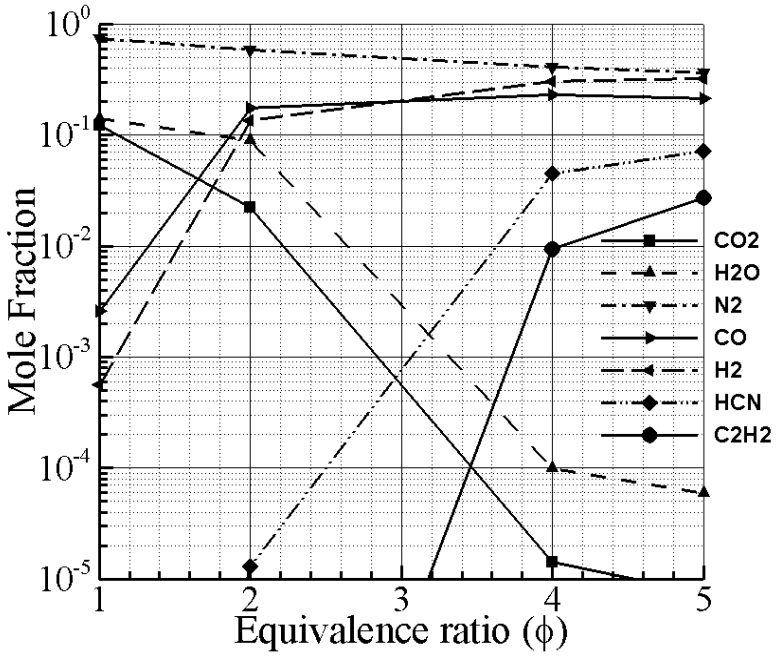

(b)

Figure 3: Effect of equivalence ratio (ϕ) on species concentration: (a) pentane, (b) n-heptane.

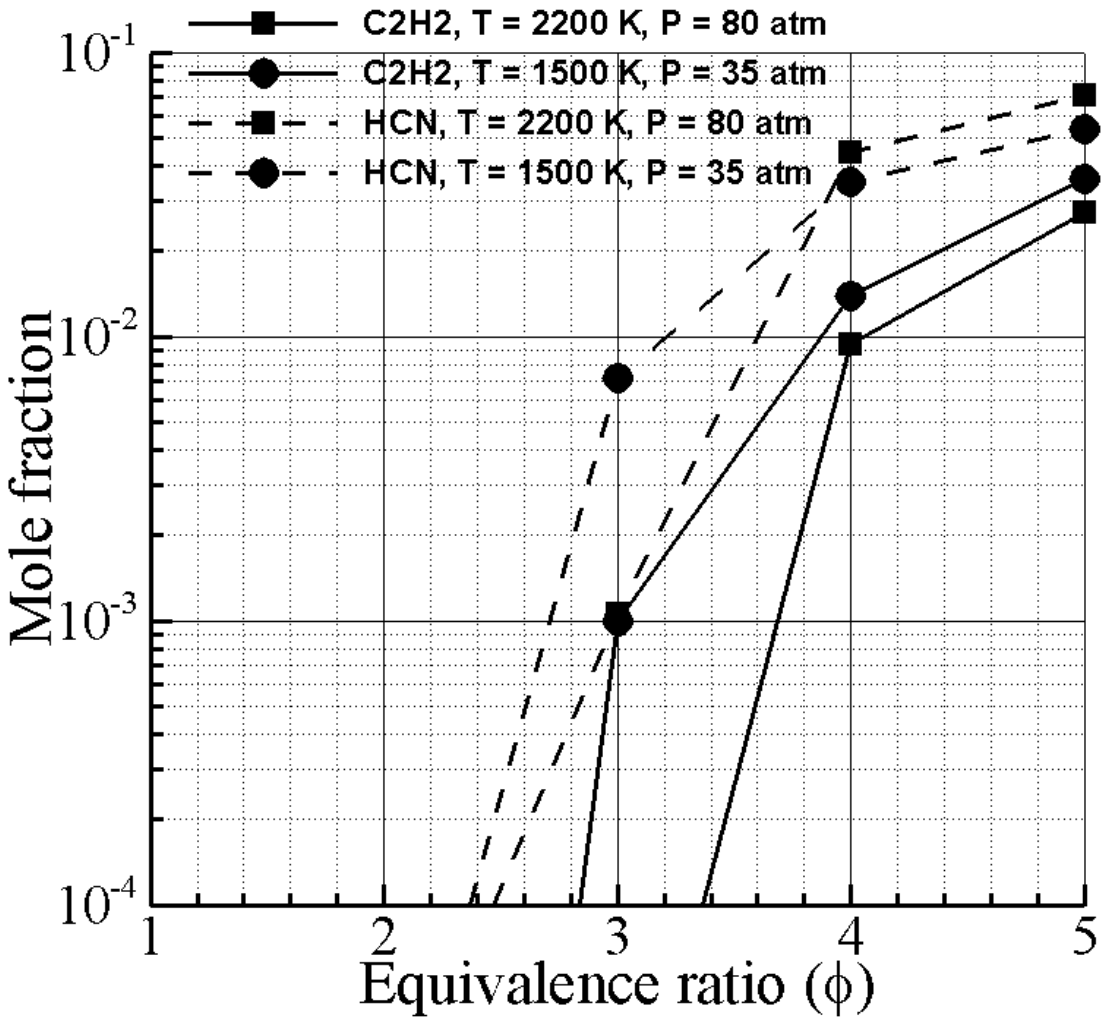

Figure 4: Effect of temperature and pressure on the formation of HCN and C_2H_2.

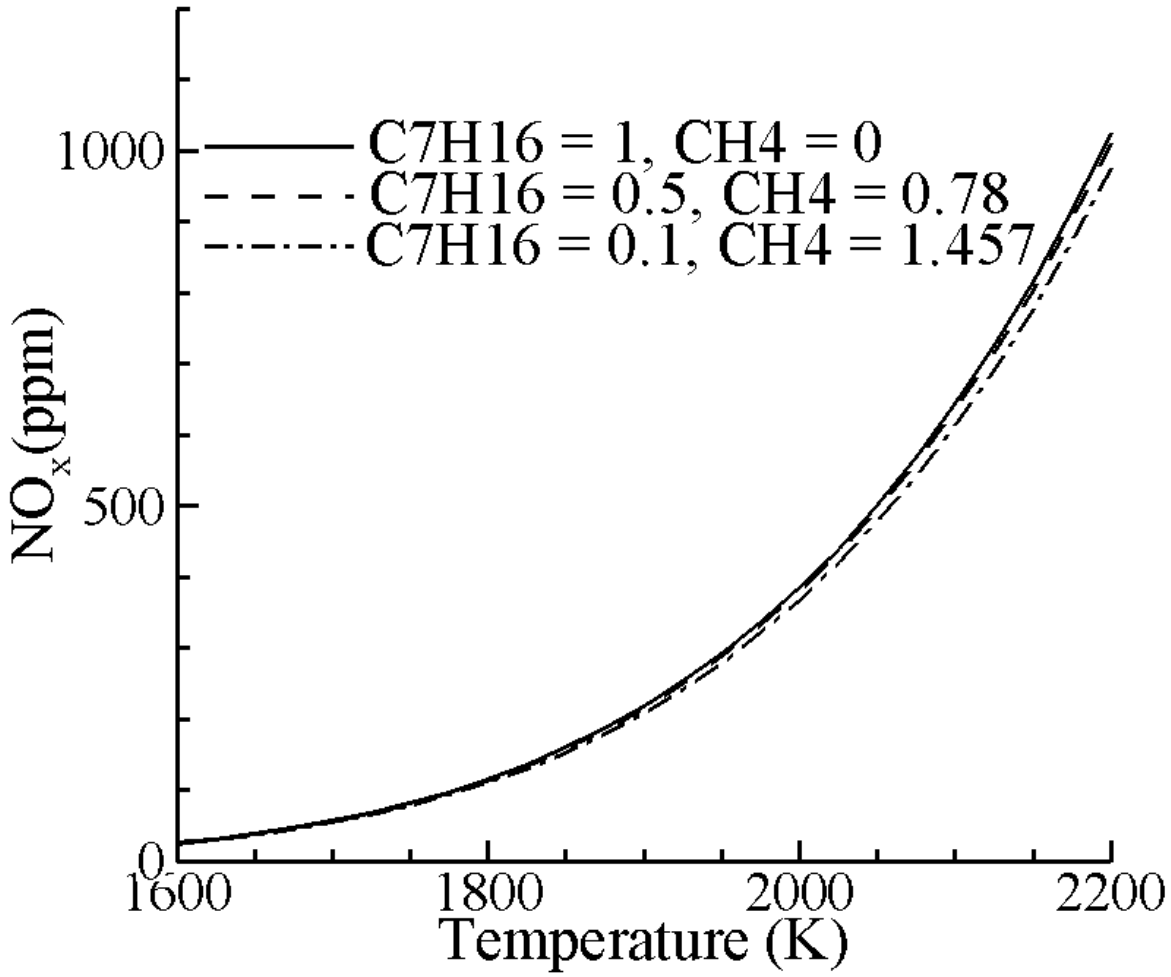

Figure 5: Variation of NO (ppm) with temperature for a natural-gas/diesel dual-fuel engine.

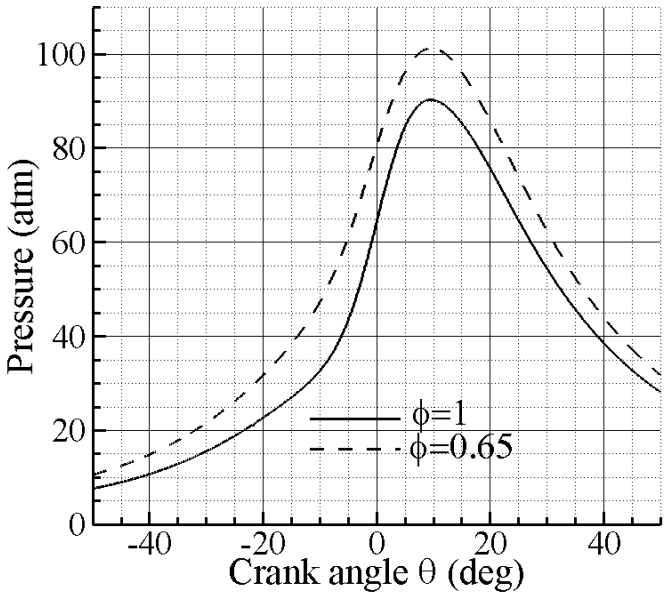

(a)

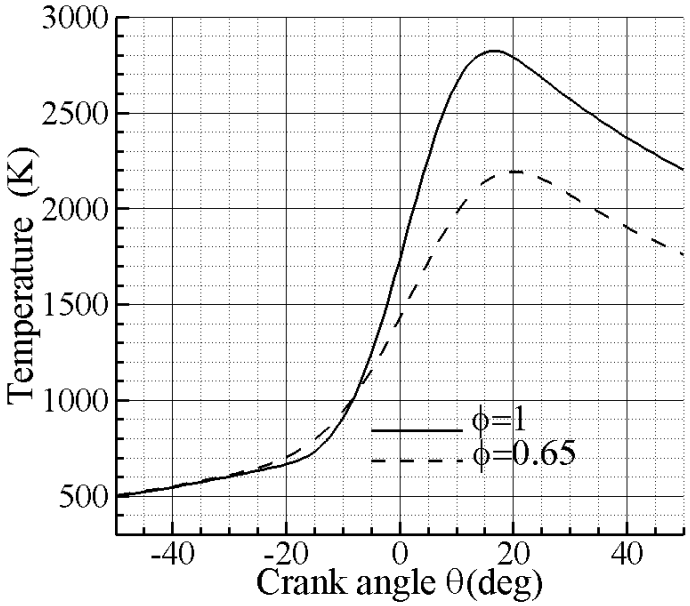

(b)

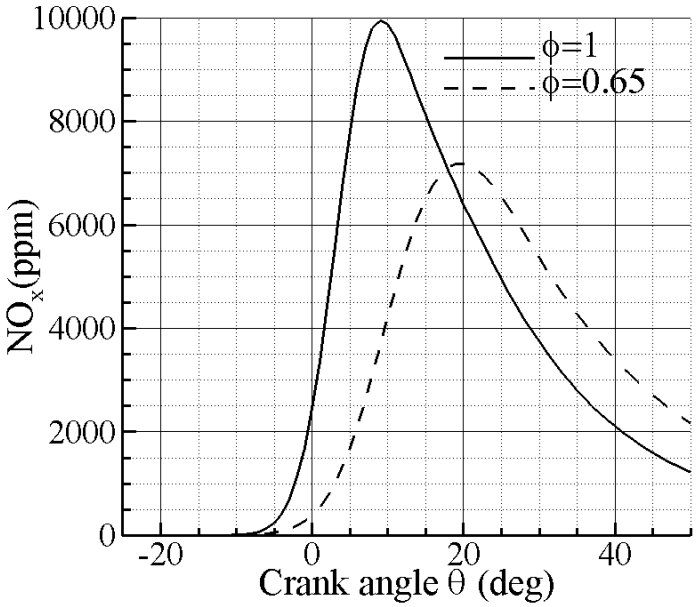

(c)

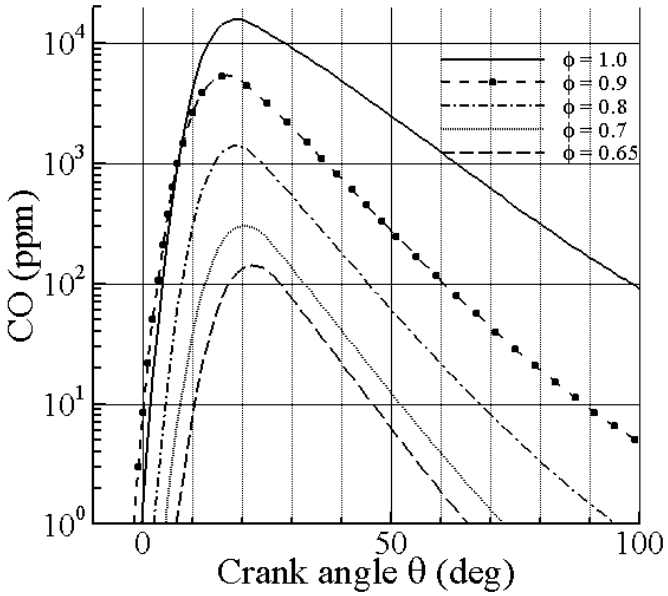

(d)

Figure 6: Temporal variation of pressure (a), temperature (b), NO (c), and CO (d) in a natural gas engine.

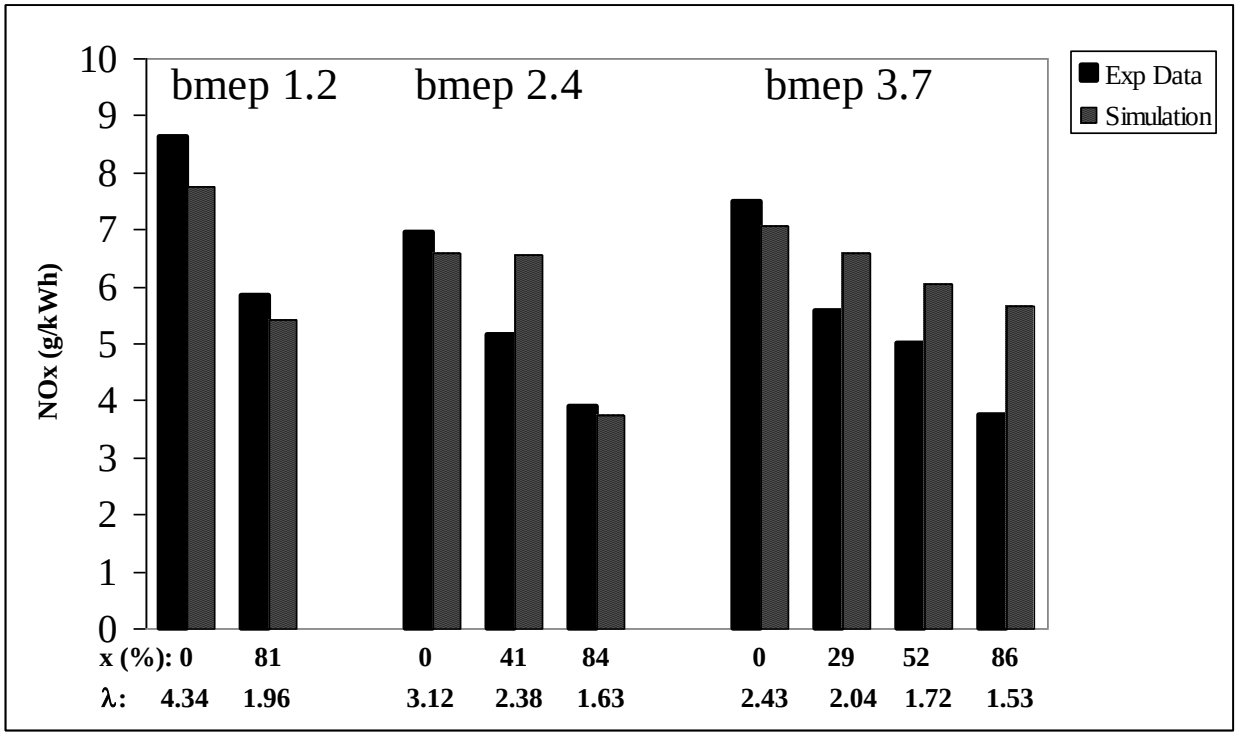

Figure 7: Comparison of predicted engine-out NO with experimental data [19].

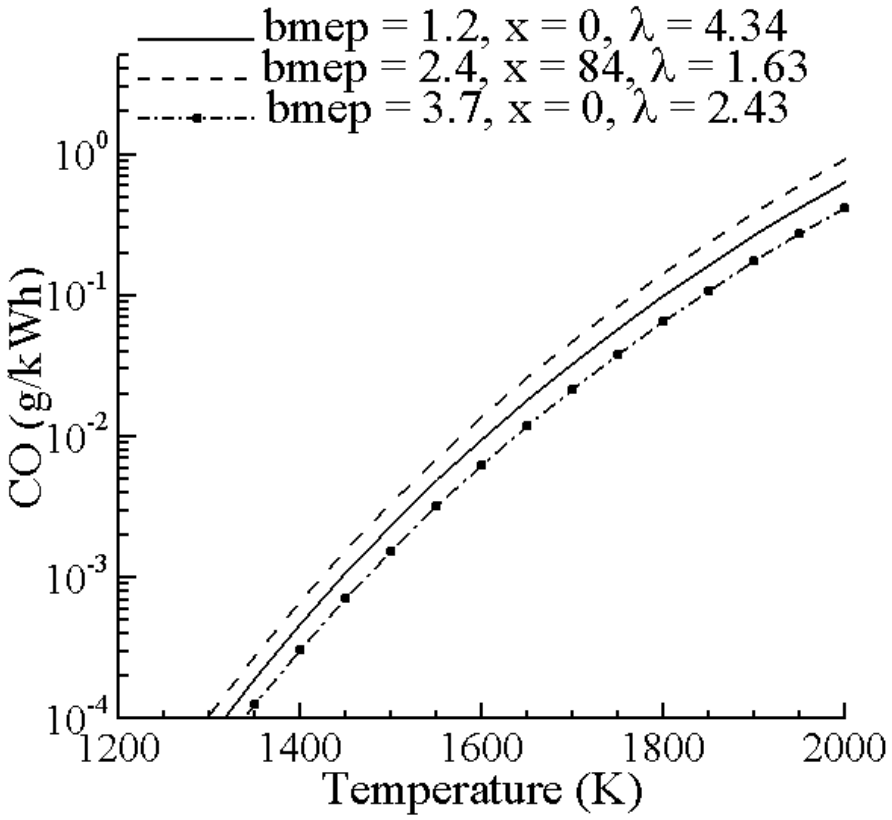

Figure 8: CO concentration for three values of load and mixture composition (x and λ).

List of Tables

List of figures: